

BISMUTH ADDITIVE NON-ISOTHERMAL CRYSTALLIZATION KINETICS OF $\text{In}_3\text{Te}_7\text{Bi}_x\text{Se}_{90-x}$

S. S. ASHRAF^{a,*}, M. ZULFEQUAR^b

^a*School of Engineering Sciences and Technology Jamia Hamdard, New Delhi-62, India*

^b*Department of Physics, Jamia Millia Islamia, New Delhi-25, India*

The present work reported the variation in kinetics parameters of chalcogenide glass of $\text{In}_3\text{Te}_7\text{Bi}_x\text{Se}_{90-x}$ ($x = 0, 5, 10, 15$) with different heating rates ($5^\circ\text{C}/\text{min}$, $10^\circ\text{C}/\text{min}$, $15^\circ\text{C}/\text{min}$, $20^\circ\text{C}/\text{min}$ and $25^\circ\text{C}/\text{min}$). Measurements of the heat flow as a function of temperature at different heating rates were carried out using Differential Scanning Calorimetry (DSC) under non-isothermal condition. Heating rate dependence of glass transition temperature (T_g), crystallization temperature (T_c) and melting temperature (T_m) were measured using DSC thermograms. Johnson-Mehl-Avrami (JMA) model was used to calculate order parameter (n). Activation energy of crystallization (ΔE_c) was calculated using Kissinger and Ozawa's equations. Activation energy for structural relaxation (ΔE_r) was determined using C.T. Moynihan et al relation. Energy Dispersive X-ray Scattering (EDS) shows the presence of compositional elements in glass alloy. Thermal Gravimetric Analysis (TGA) was carried to measure the temperature above which weight loss of the materials begins. Scanning Electron Microscope (SEM) image depicts surface topology and nuclei growth. X-ray Diffraction (XRD) of alloys was carried out to analyze the amorphous or polycrystalline behavior of the alloy. Based on kinetics parameters of the glass studied, it is found that difference in crystallization temperature and glass transition temperature is maximum and enthalpy of crystallization (ΔH_c) is minimum for $\text{In}_3\text{Te}_7\text{Bi}_{10}\text{Se}_{80}$ glass. Therefore, this glass is more stable and hence can be used in photolithography, xerography, switching and optical memory devices.

(Received August 8, 2019; Accepted December 9, 2019)

Keywords: Chalcogenide, DSC, Crystallization, Activation Energy, Enthalpy

1. Introduction

Chalcogenide glasses are inorganic glassy materials of Group IV of the periodic table which contain one or more chalcogen elements such as Se, Te, S. Se-based chalcogenide glasses have been promising materials for its applications in electronics, opto-electronic, xerography and other solid state devices [1-5]. Since pure selenium has many shortcomings such as short lifetime, low thermal stability, therefore certain additives are used to overcome these shortcomings. Se-Te, Se-In, Se-Bi alloys are of great interest owing to their properties of high sensitivity, greater hardness. These materials have the properties of changing phase from amorphous also called non-crystalline phase to crystalline phase on instantly cooling and heating. They have unique properties of reversible transformation. Because of its phase change properties, they have wide applications in solid state and optical storage devices [6-8]. In amorphous phase atoms are not arranged in regular fashion. They lack long range order. The process of reorganization of the atomic structure is called structural relaxation and is classified according to the property that is being observed such as enthalpy relaxation [9-11].

In this present work, the author aims to study the crystallization kinetics by determining kinetics parameters using DSC under non-isothermal condition. The glass transition temperature (T_g), crystallization temperature (T_c) and melting temperature (T_m) have been determined by DSC thermograms. The activation energies for crystallization (ΔE_c) have been determined using

* Corresponding author: shahabash@gmail.com

Kissinger [12-15] and Ozawa equations [16]. Activation energy for structural relaxation (ΔE_t) was determined using C.T. Moynihan et al relation [17]. Avrami exponent was obtained from JMA model [18]. The phases crystallized were determined using X-ray diffraction (XRD) and scanning electron microscopy (SEM). In the present bulk alloys of $\text{In}_3\text{Te}_7\text{Bi}_x\text{Se}_{90-x}$, on increasing the concentration of bismuth the glass transition temperature and crystallization temperature increase due to increase in cohesive energy and hence glass forming tendency increases [19-21]. Bismuth doped chalcogenide glasses have become attractive materials due to their potential applications in optoelectronic devices [22-25]. Quaternary chalcogenide glasses exhibit two and three dimensional growth as it expands the glass forming area and creates compositional and configurationally disorder [26-27]. Te based chalcogenide glasses have applications in optical memory devices such as rewritable digital versatile disks [28]. Several researchers reported crystallization kinetics of selenium, tellurium, bismuth and indium based ternary and quaternary chalcogenide glasses and its applications [29-37].

2. Experimental

Glassy alloys of $\text{In}_3\text{Te}_7\text{Bi}_x\text{Se}_{90-x}$ ($x = 0, 5, 10$ and 15) were prepared from high purity constituent elements (99.999%) in stoichiometric ratio by using melt quench technique. The constituent elements were sealed in quartz ampoules under a vacuum of 10^{-6} torr. The ampoule was kept inside a furnace at 900°C for 10 hrs so that all elements were melted. The temperature was raised at the rate of $3^\circ\text{C}/\text{min}$. During the heating process, the ampoule was shaken continuously so as to make it homogeneous. Quenching was done in ice water and the ingots were taken out by breaking the ampoule. The X-ray diffraction (XRD) patterns give the important information about the nature and structure of the samples. Glassy alloys surface topography and composition have been studied by SEM image and EDS respectively.

DSC technique was used to determine the kinetic parameters of the glassy alloy at five different heating rates i.e. $5^\circ\text{C}/\text{min}$, $10^\circ\text{C}/\text{min}$, $15^\circ\text{C}/\text{min}$, $20^\circ\text{C}/\text{min}$ and $25^\circ\text{C}/\text{min}$. DSC was done using TA instruments Q-200 Differential Scanning Calorimetry (Temp precision $\pm 0.5^\circ\text{C}$, Sensitivity $-0.2 \mu\text{W}$). Thermal Gravimetric Analysis (TGA) was carried out by TA Instruments Q-500 to analyze the weight loss (%) of the sample with temperature.

3. Results and discussion

XRD analysis of bulk glass alloy was carried out by A Regaku Ultima IV X-ray Diffractometre. The radiation source $\text{Cu K}\alpha_1$ with $\lambda = 1.54 \text{ \AA}$, diffraction angle in the range of 5° to 90° with scan speed of $2^\circ/\text{min}$ and a chart speed of $1 \text{ cm}/\text{min}$ were maintained. The pattern of graph is shown in Fig 1. The XRD diffractograms show that the Bi-rich samples ($x > 10\%$) have some extent crystallization peaks due to the presence of other phase of the material in Bi-rich samples. Amorphous nature of the $\text{In}_3\text{Te}_7\text{Bi}_x\text{Se}_{90-x}$ glass alloys decreases with increase of Bi concentration. Surface morphology of the thin film was analysed by Scanning Electron Micrograph (SEM) apparatus JEOL (Model JSM 6380). SEM image of bulk alloy is shown in Fig 2. SEM image shows the growth of nuclei. The dissociation energy for Se-In, Se-Se, Se-Te, Bi-Bi, Bi-Se, Bi-Te and Bi-In are 257.5 KJ/mol , 239.3 KJ/mol , 259.8 KJ/mol , 200.4 KJ/mol , 280.3 KJ/mol , 232.3 KJ/mol and 2018.0 KJ/mol respectively [38]. This shows that Se-Bi bonds require more energy to be dissociated which makes it robust. Bismuth has greater affinity for selenium than tellurium. This shows that Bi-Se bonds require more energy to be dissociated which makes it robust.

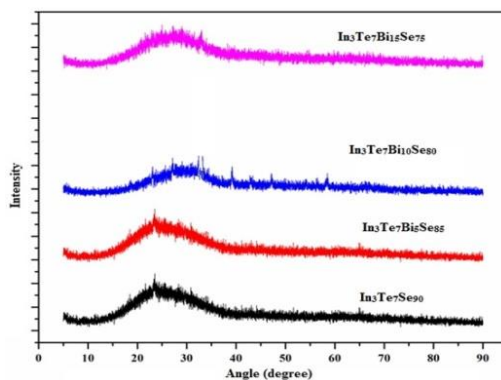


Fig.1.XRD pattern of $\text{In}_3\text{Te}_7\text{Bi}_x\text{Se}_{90-x}$ ($x = 0, 5, 10, 15$) powder.

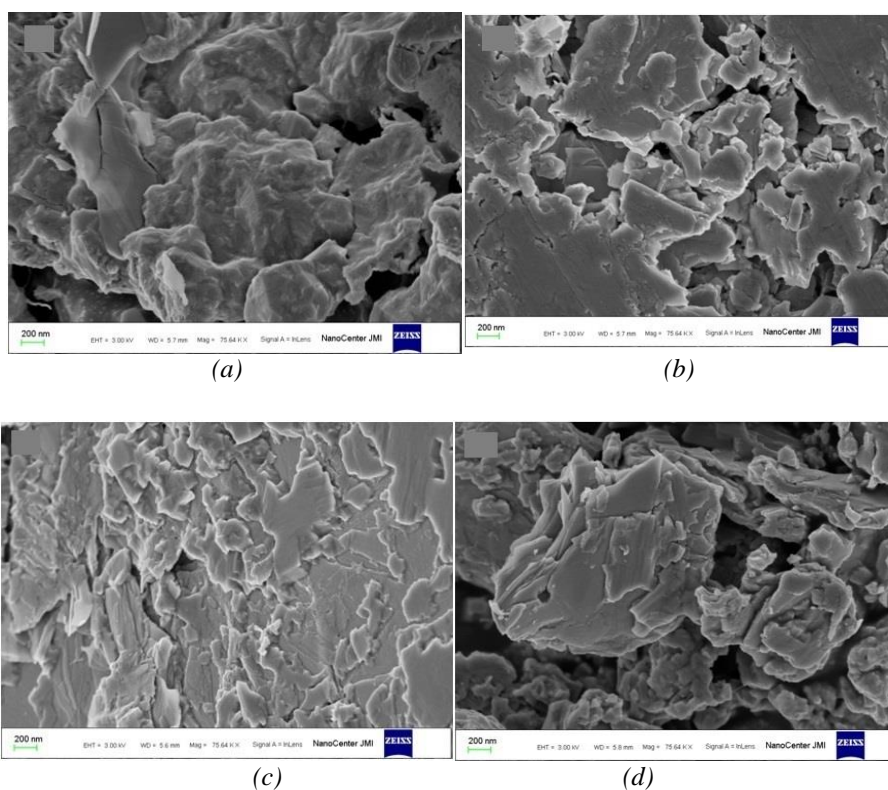


Fig. 2 SEM images of (a) $\text{In}_3\text{Te}_7\text{Se}_{90}$ (b) $\text{In}_3\text{Te}_7\text{Bi}_5\text{Se}_{85}$ (c) $\text{In}_3\text{Te}_7\text{Bi}_{10}\text{Se}_{80}$ and (d) $\text{In}_3\text{Te}_7\text{Bi}_{15}\text{Se}_{75}$ bulk alloys.

The elemental composition of as-prepared $\text{In}_3\text{Te}_7\text{Bi}_x\text{Se}_{90-x}$ ($x = 0, 5, 10, 15$) bulk alloys are checked by using the Energy Dispersive X-ray (EDX) spectroscopy. Fig.3. shows the typical EDX patterns of as-prepared thin films of $\text{In}_3\text{Te}_7\text{Bi}_x\text{Se}_{90-x}$ ($x = 0, 5, 10, 15$). This image confirms the presence of constituent's elements In, Te, Bi and Se. The calculated wt% values show Se (96.08%), Te (2.98%) and In (0.08%) for $\text{In}_3\text{Te}_7\text{Se}_{90}$, Se (84.43%), Te (2.27%), In (0.17%) and Bi (13.13%) for $\text{In}_3\text{Te}_7\text{Bi}_5\text{Se}_{85}$. Similarly the wt% values of other compositions agree well with experimentally taken wt% values. Intense peaks for Se found in the spectra of all samples are due to its high concentration as compared to other constituent such as In, Te and B.

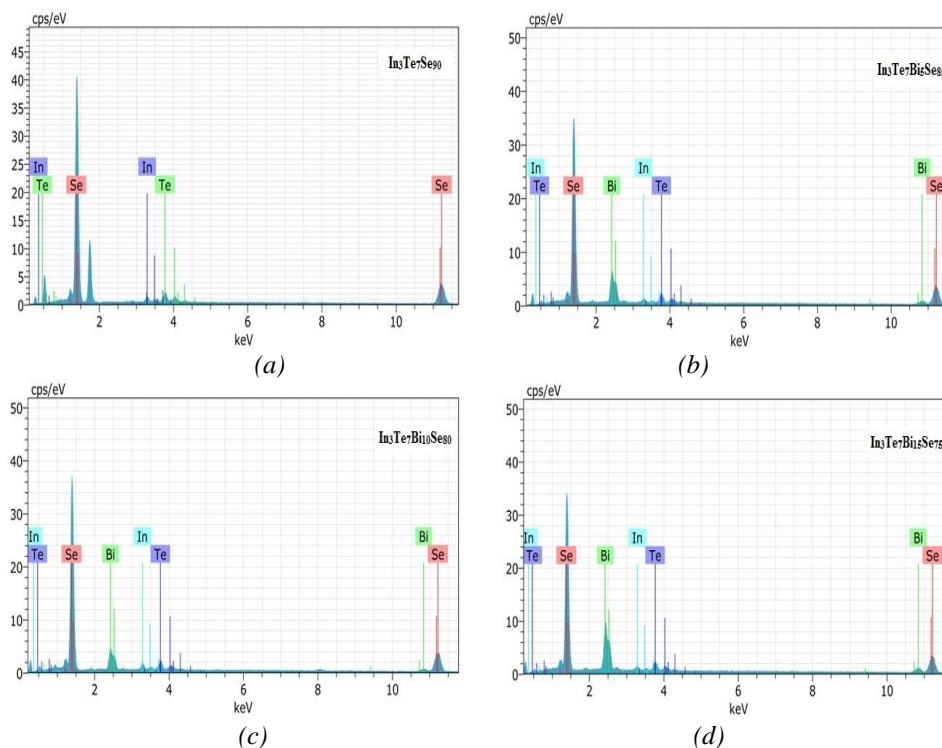


Fig. 3. Energy Dispersive X-ray Spectroscopy (EDS) of $\text{In}_3\text{Te}_7\text{Bi}_x\text{Se}_{90-x}$ ($x = 0, 5, 10, 15$) bulk alloys.

The thermal analysis of $\text{In}_3\text{Te}_7\text{Bi}_x\text{Se}_{90-x}$ ($x = 0, 5, 10, 15$) bulk alloys was carried out by using DSC in the temperature range from 25°C to 250°C and at five different heating rates i.e. $5^\circ\text{C}/\text{min}$, $10^\circ\text{C}/\text{min}$, $15^\circ\text{C}/\text{min}$, $20^\circ\text{C}/\text{min}$ and $25^\circ\text{C}/\text{min}$. The amount of 8-10 milligrams of sample is heated at a constant heating rate and changes in heat flow with respect to empty aluminum pan were measured. DSC thermograms for $\text{In}_3\text{Te}_7\text{Bi}_x\text{Se}_{90-x}$ ($x = 0, 5, 10, 15$) bulk alloys at five heating rates ie $5^\circ\text{C}/\text{min}$, $10^\circ\text{C}/\text{min}$, $15^\circ\text{C}/\text{min}$, $20^\circ\text{C}/\text{min}$ and $25^\circ\text{C}/\text{min}$ are shown in Fig.4. It is clear from the characteristics of graph that glass transition temperature (T_g) and crystallization temperature (T_c) vary with heating rates. Glass transition temperature (T_g) and crystallization temperature (T_c) increase with increasing heating rates for all samples as shown in Table 1 (a) & (b).

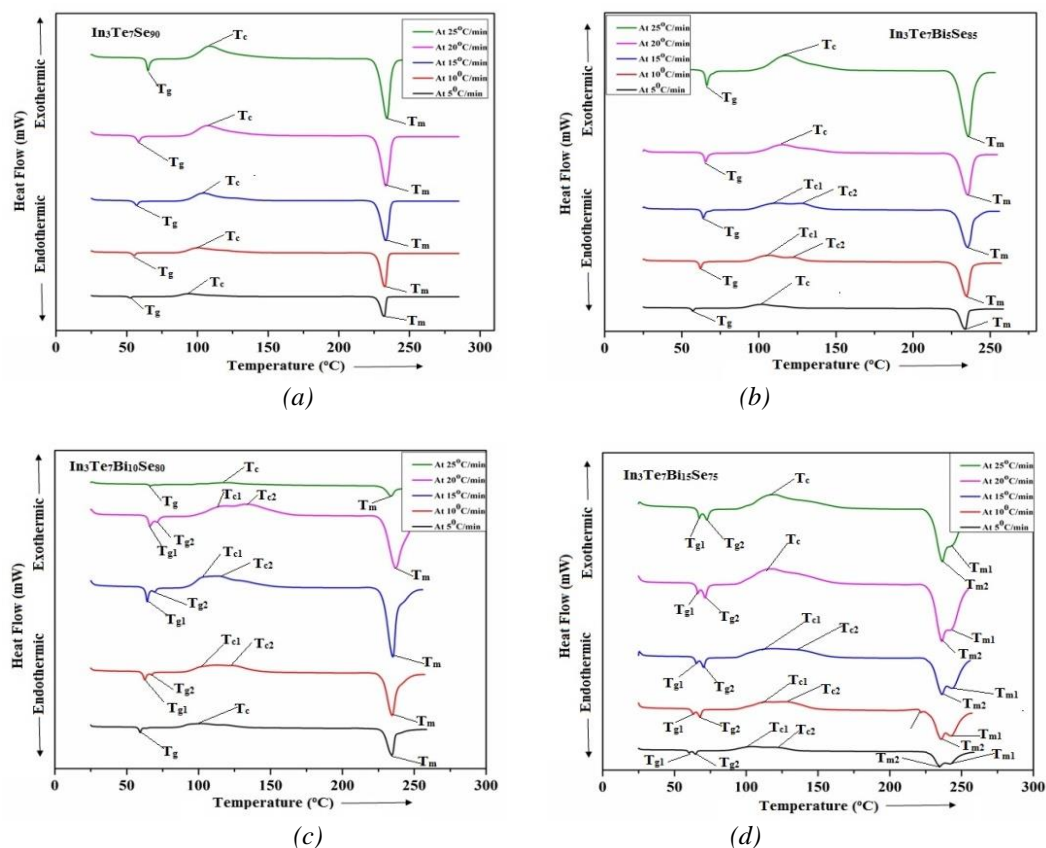


Fig. 4. DSC thermograms for (a) $\text{In}_3\text{Te}_7\text{Se}_{90}$ (b) $\text{In}_3\text{Te}_7\text{Bi}_5\text{Se}_{85}$ (c) $\text{In}_3\text{Te}_7\text{Bi}_{10}\text{Se}_{80}$ and (d) $\text{In}_3\text{Te}_7\text{Bi}_{15}\text{Se}_{75}$ bulk alloys.

Table 1(a). Heating rate dependence of glass transition temperature and crystallization temperature for $\text{In}_3\text{Te}_7\text{Se}_{90}$ and $\text{In}_3\text{Te}_7\text{Bi}_5\text{Se}_{85}$.

S.No.	Heating Rate ($^{\circ}\text{C}/\text{min}$)	$\text{In}_3\text{Te}_7\text{Se}_{90}$			$\text{In}_3\text{Te}_7\text{Bi}_5\text{Se}_{85}$		
		T_g (K)	T_c (K)	$T_c - T_g$ (K)	T_g (K)	T_c (K)	$T_c - T_g$ (K)
1	5	325.9	367.1	41.2	330.4	375.3	44.9
2	10	328.5	374.2	45.7	335.3	380.7	45.4
3	15	330.2	377.6	47.4	337.2	385.5	48.3
4	20	331.5	380.5	49.0	338.5	388.3	49.8
5	25	338.2	381.9	43.7	339.3	390.6	51.3

Table 1(b). Heating rate dependence of glass transition temperature and crystallization temperature for $\text{In}_3\text{Te}_7\text{Bi}_{10}\text{Se}_{80}$ and $\text{In}_3\text{Te}_7\text{Bi}_{15}\text{Se}_{75}$.

S.No.	Heating Rate ($^{\circ}\text{C}/\text{min}$)	$\text{In}_3\text{Te}_7\text{Bi}_{10}\text{Se}_{80}$			$\text{In}_3\text{Te}_7\text{Bi}_{15}\text{Se}_{75}$		
		T_g (K)	T_c (K)	$T_c - T_g$ (K)	T_g (K)	T_c (K)	$T_c - T_g$ (K)
1	5	332.5	375.3	42.8	337.9	377.1	39.2
2	10	335.6	386.1	50.5	341.0	399.9	58.9
3	15	337.4	385.6	48.2	343.4	391.8	48.4
4	20	339.4	407.3	67.9	344.5	391.2	46.7
5	25	339.5	394.2	54.7	345.7	392.3	46.6

As shown in the above Table 1(a) and Table 1(b), glass transition temperature T_g increases with increasing bismuth concentration at different heating rates. It leads to increasing of lattice rigidity. T_g represents the strength of the rigidity of the glass structure [39]. Since glass transition temperature (T_g) increases with incorporation of bismuth in In-Te-Se system therefore, it can be suggested that the rigidity of the investigated glassy system In-Te-Bi-Se increases with bismuth content. On the basis of short range order concept, the increase in T_g can be attributed to the decrease in the dimensionality of the structural units [40-42]. T_g is heating rate dependent as observed and shown in Table 1 (a) & (b). The results are in tune with those obtained by K.A. Aly et al. [43] and E.R. Shabaan et al. [44]. The supercooled region of an amorphous alloy T_c - T_g is widely used to characterize the thermal stability of these materials. The results present in the table shows that T_c - T_g are heating rate dependants. The higher value of T_c - T_g is obtained for $\text{In}_3\text{Te}_7\text{Bi}_{10}\text{Se}_{80}$ at heating rate $20^\circ\text{C}/\text{min}$ sample (shown in Fig.5), which shows the good thermal stable alloy.

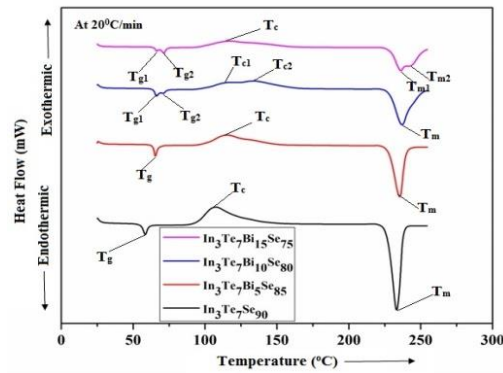


Fig.5 DSC thermograms for $\text{In}_3\text{Te}_7\text{Bi}_x\text{Se}_{90-x}$ ($x = 0, 5, 10, 15$) bulk alloys at heating rate $20^\circ\text{C}/\text{min}$.

The two values of glass transition temperature (T_{g1} , T_{g2}) indicate two different phases of material. This should be the case like a random copolymer. In copolymer phase such kind of transition is expected [45]. Two values of peak crystallization temperature (T_{c1} , T_{c2}) suggest that glass may crystallize into two different phases. Two melting points T_{m1} and T_{m2} in sample alloy $\text{In}_4\text{Se}_{84}\text{S}_{12}$ shows partial melting and recrystallization of crystallite at the moment of thermal scanning [46]. The two peaks for T_g , T_c and T_m are observed as the Bi concentration increases, $x > 10$ at %.

Crystallization kinetics of amorphous semiconductor has been studied using Johnson-Mehl-Arvami (JMA) model [47-49] in which crystallization fraction (α) as a function of time is expressed as

$$\alpha(t) = 1 - \exp[-(kt)^n] \quad (1)$$

Where $\alpha(t)$ is the volume fraction crystallized after time t and n is the Avrami exponent rate constant encompassing nucleation and crystal growth factor whose temperature dependence is generally expressed by the Arrhenian-type equation [17-19]

$$k = k_0 \exp(-E/RT) \quad (2)$$

where k_0 is the frequency factor, E is the apparent activation energy for crystallization, R is the ideal gas constant and T is the temperature in kelvin.

In a non-isothermal DSC measurements, the temperature is changed linearly with time at a rate β ($=dT/dt$).

$$T = T_0 + \beta t \quad (3)$$

Where T_0 is the initial temperature and T is the temperature after time t . As the temperature constantly changes with time, k is no longer a constant but varies with time in a more complicated from the Eq. (1) becomes

$$\alpha(t) = 1 - \exp[-\{k(T - T_0)/\beta\}^n] \quad (4)$$

after rearranging and taking double logarithms of Eq.(4) becomes

$$\ln[-\ln(1 - \alpha)] = \ln k(T - T_0) - n \ln \beta \quad (5)$$

From the Eq. (5), a plot between $\ln[-\ln(1 - \alpha)]$ versus $\ln \beta$ yields a straight line with slope equal to n (order parameter). Fig.7 shows the variation of $\ln[-\ln(1 - \alpha)]$ against $\ln \beta$ for $\text{In}_3\text{Te}_7\text{Bi}_x\text{Se}_{90-x}$ ($x = 0, 5, 10, 15$) at 105°C . The value of n for the different compositions is given in Table 2. Since as-quenched sample is studied, the value of m is taken as $m = n - 1$ [50]. The value of m is unity for binary, two for ternary samples and three for quaternary glasses indicating dimensional growth of the samples [51-53]. The value of Avrami index n depending on the crystallization mechanism, $n = 4$ represents volume nucleation with 3-D growth, $n = 3$ represents volume nucleation with 2-D growth, $n = 2$ represents volume nucleation with 1-D growth and $n = 1$ represents surface nucleation with 1-D growth from the surface to the inside of the sample [51]. The values of Avrami index n observed are 2.76, 3.68, 3.73 and 3.87 for different concentration of Bi in $\text{In}_3\text{Te}_7\text{Bi}_x\text{Se}_{90-x}$. The non-integer values of n indicate two crystallization mechanisms (2-D and 3-D) are observed during the amorphous to crystalline transformation in the $\text{In}_3\text{Te}_7\text{Bi}_x\text{Se}_{90-x}$ ($x = 0, 5, 10, 15$) with component chalcogenide glasses.

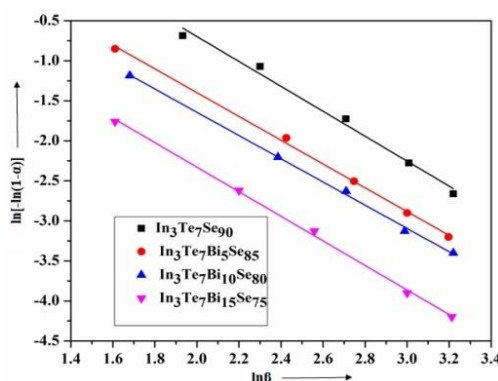


Fig. 7. Plot between $\ln[-\ln(1 - \alpha)]$ versus $\ln \beta$ for $\text{In}_3\text{Te}_7\text{Bi}_x\text{Se}_{90-x}$ ($x = 0, 5, 10, 15$) alloys.

Table 2. Value of Avrami exponent for a - $\text{In}_3\text{Te}_7\text{Bi}_x\text{Se}_{90-x}$ ($x = 0, 5, 10, 15$) at 105°C .

S.No.	Sample	n	m
1	$\text{In}_3\text{Te}_7\text{Se}_{90}$	2.76	2
2	$\text{In}_3\text{Te}_7\text{Bi}_5\text{Se}_{85}$	3.68	3
3	$\text{In}_3\text{Te}_7\text{Bi}_{10}\text{Se}_{80}$	3.73	3
4	$\text{In}_3\text{Te}_7\text{Bi}_{15}\text{Se}_{75}$	3.87	3

The heating rate (β) dependence up on the glass transition T_g in chalcogenide glasses may be interpreted in terms of thermal relaxation phenomena and it has been shown by Moynihan et al [54-55] that the activation energy of structural relaxation (ΔE_t) can be related to T_g and β by

$$\frac{d \ln \beta}{d \left(\frac{1}{T_g} \right)} = - \frac{\Delta E_t}{RT_g} \quad (8)$$

From the above equation we can conclude that plot of $\ln\beta$ vs $1000/T_g$ should be straight line and the slope gives activation energy of structural relaxation (ΔE_t).

Fig 8 shows the graph $\ln\beta$ vs $1000/T_g$ for all four samples a- $\text{In}_3\text{Te}_7\text{Bi}_x\text{Se}_{90-x}$ ($x = 0, 5, 10, 15$) which comes to be a straight line. The value of activation energy of structural relaxation (ΔE_t) can be calculated from the slope of these straight lines as shown in Table 3. It is clear from this table that the value of ΔE_c and ΔE_t increases monotonically with the increasing bismuth content. The present crystallization study shows that ΔE_c and ΔE_t increases as bismuth concentration increases which also indicate that the rate of crystallization is fast in bismuth incorporated alloys than in alloys with small bismuth content.

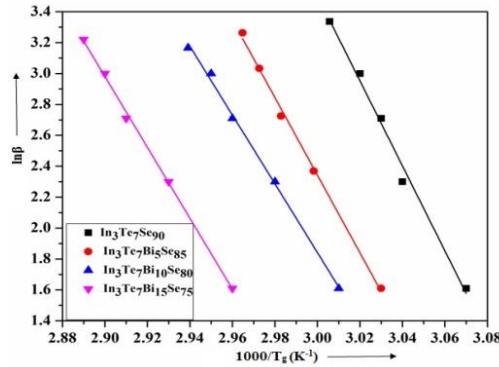


Fig.8. Plot between $\ln\beta$ versus $1000/T_g$ for $\text{In}_3\text{Te}_7\text{Bi}_x\text{Se}_{90-x}$ ($x = 0, 5, 10, 15$) alloys.

The activation energy of crystallization ΔE_c can be obtained from the variation of the onset crystallization temperature T_c with heating rate by using Ozawa Equation [56-57] as

$$\ln \beta = -\Delta E_c / RT_c + C \quad (6)$$

Where C is a constant and R is a gas constant.

Fig.9 shows $\ln\beta$ versus $1000/T_c$ curves, which come to be linear for the entire heating rate. The value of ΔE_c is calculated from the slope of each curve.

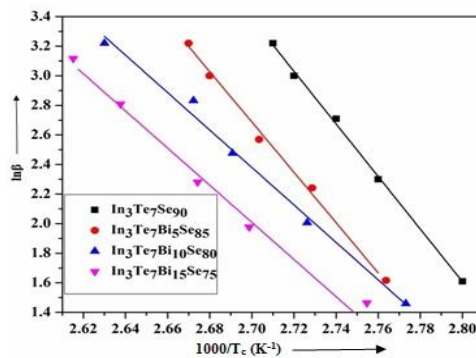


Fig.9. Plot between $\ln\beta$ versus $1000/T_c$ for $\text{In}_3\text{Te}_7\text{Bi}_x\text{Se}_{90-x}$ ($x = 0, 5, 10, 15$) alloys.

These values of ΔE_c for all the samples of $\text{In}_3\text{Te}_7\text{Bi}_x\text{Se}_{90-x}$ ($x = 0, 5, 10, 15$) are shown in Table 3

The interpretation of the experimental crystallization data is given on the basis of Kissinger's [58] and Matusia's equations for the non-isothermal crystallization [59]. The activation energy (ΔE_c) for crystallization can also be calculated by using Kissinger's equation

$$\ln(\beta/T_c^2) = -\Delta E_c/RT_c + D \quad (7)$$

The plot of $\ln(\beta/T_c^2)$ versus $1000/T_c$ for all the sample are shown in Fig.10 which appears to be straightlines. The value of ΔE_c may be calculated from the slope of each curve. The values of ΔE_c for all the samples of a- $\text{In}_3\text{Te}_7\text{Bi}_x\text{Se}_{90-x}$ ($x = 0, 5, 10, 15$) alloy sare shown in Table 3.

The ΔE_c of crystallization is an indication of the speed of the rate of crystallization. It is useful for the characterization of glassy alloys for different applications. It is clear from the Table 3 that the value of ΔE_c is maximum for $\text{In}_3\text{Te}_7\text{Bi}_{15}\text{Se}_{75}$ which indicates that the speed of rate of crystallization is faster in that sample.

The value of ΔE_c obtained by the above two theories are in good agreement to each other

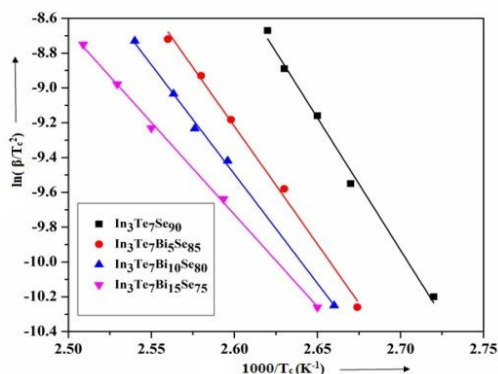


Fig. 10. plot of $\ln(\beta/T_c^2)$ versus $1000/T_c$ for $\text{In}_3\text{Te}_7\text{Bi}_x\text{Se}_{90-x}$ ($x = 0, 5, 10, 15$) alloys.

Table 3. Activation Energy for structural relaxation and activation energy of crystallization.

Sample	ΔE_t (kJ/mol)	ΔE_c (kJ/mol)	ΔE_c (kJ/mol)
		From Ozawa's relation ($\ln\beta$ vs $1000/T_c$)	From Kissinger's equation ($\ln\beta/T_c^2$ vs $1000/T_c$)
$\text{In}_3\text{Te}_7\text{Se}_{90}$	34.2	38.2	36.1
$\text{In}_3\text{Te}_7\text{Bi}_5\text{Se}_{85}$	37.9	42.7	39.8
$\text{In}_3\text{Te}_7\text{Bi}_{10}\text{Se}_{80}$	39.1	43.3	41.4
$\text{In}_3\text{Te}_7\text{Bi}_{15}\text{Se}_{75}$	43.3	45.6	43.9

It has been reported that chalcogenide glass rich in Se content mostly contains about 40% Se atoms in ring structure and 60% of Se atoms in polymeric chains. Selenium glass consists of a mixture of long chains and Se rings. The incorporation of In, Te and Bi decreases the number of Se rings and increases the number of long Se-Bi-In-Te polymeric chains and Se-Bimixed rings, thus makes the Se-Bi-In-Te system more rigid and a higher activation energy is needed for molecular motions and rearrangements near the T_g . As the bismuth content increases, the possibility of Bi-Bi/Se-Bi bond may be aroused and hence increases the density of state.

The crystallization Enthalpy (ΔH_c) was calculated for all samples of $\text{In}_3\text{Te}_7\text{Bi}_x\text{Se}_{90-x}$ ($x = 0, 5, 10$, and 15) using the formula:

$$\Delta H_c = \frac{kA}{m} \quad (8)$$

Where, $k = 1.5$ is the constant of the instrument used. The value of “ k ” was calculated by measuring the total area of the complete melting endothermic peak of high-purity Indium and Tin and used the well –known enthalpy of melting of these standard materials. The area of crystallization peak is “ A ” and “ m ” is the mass of the materials used. The value of the ΔH_c for

various samples of $\text{In}_3\text{Te}_7\text{Bi}_x\text{Se}_{90-x}$ ($x = 0, 5, 10, 15$) at different heating rates are given in Table 4. The enthalpy release is related to the meta – stability of the glasses. It is clear from the Table 4 that minimum heat is released for the composition with 15% of Bi, which confirms the maximum stability of the glass.

Table 4. Crystallisation enthalpy of the alloys at different heating rates.

Sample	$\Delta H_c(\text{J/g})$				
	At 5 °C /min	At 10°C /min	At 15 °C /min	At 20°C /min	At 25°C /min
$\text{In}_3\text{Te}_7\text{Se}_{90}$	41.9	44.4	45.1	44.7	43.0
$\text{In}_3\text{Te}_7\text{Bi}_5\text{Se}_{85}$	36.8	36.4	35.1	27.2	39.0
$\text{In}_3\text{Te}_7\text{Bi}_{10}\text{Se}_{80}$	31.4	34.3	36.1	16.7	21.2
$\text{In}_3\text{Te}_7\text{Bi}_{15}\text{Se}_{75}$	22.0	22.9	21.2	23.7	17.1

4. Conclusions

Crystallisation kinetics of chalcogenide glass $\text{In}_3\text{Te}_7\text{Bi}_x\text{Se}_{90-x}$ ($x = 0, 5, 10, 15$) alloys at different heating rates under non-isothermal conditions have been studied. The samples are characterized by XRD, SEM and EDS techniques for finding the nature, structure, morphology and constituents materials. EDS analysis confirms the presence of constituents elements in the alloys. Avrami exponent (n) has been measured using JMA model. Kissinger and Ozawa equations have been used to determine Activation Energy (ΔE_c) of Crystallization. It is found that the values of ΔE_c determined by both techniques are in agreement with each other. ΔE_c varies with composition indication a structural change due to addition of bismuth. The temperature difference $T_c - T_g$ is maximum for sample $\text{In}_3\text{Te}_7\text{Bi}_{10}\text{Se}_{80}$ and crystallization enthalpy (ΔH_c) is minimum for the same. This indicates that this glass is thermally most stable. The activation energy of structural relaxation (ΔE_t) increases with increasing percentage of bismuth content. The additional Bi atom is incorporated in cross-linking the Se chains by bonding with Se atoms. Further addition of Bi leads to a breaking of the chains and the formations of a large number of smaller chains.

Acknowledgements

We are thankful to SMITA Lab, Indian Institute of Technology (IIT) Delhi, New Delhi for rendering help in carrying out DSC and TGA experiments and Centre for Nanoscience and Technology, Jamia Millia Islamia, New Delhi for XRD, SEM and EDS characterization of the materials.

References

- [1] D. Lezal, J. Optoelectron. Adv. M. **5**(1), 23 (2003).
- [2] Inoue, Masayoshi, Shoji Tsuchihashi, Yoji Kawamoto, Vitreous photoconductive material, U.S. Patent 3,962,141, issued June 8, 1976.
- [3] N. Mehta, Applications of chalcogenide glasses in electronics and optoelectronics: a review, (2006).
- [4] K. Sharma, M. LAL, N. Goyal. J. Opto. Bio. Mat. **6**, 27 (2014).
- [5] Mehta, Neeraj, Ashok Kumar, Recent Patents on Materials Science **6**(1), 59 (2013).
- [6] Bureau, Bruno, Catherine Boussard-Pledel, Pierre Lucas, Xianghua Zhang, Jacques Lucas. Molecules **14**(11), 4337 (2009).
- [7] Svoboda, Roman, Miloš Krbal, Jiří Málek. Journal of Non-Crystalline Solids **357**(16-17), 3123(2011).
- [8] M. Popescu, J. Optoelectron. Adv. M. **7**(4), 2189 (2005).
- [9] Svoboda Roman, Acta Materialia **61**(12), 4534 (2013).

- [10] A. H. Abou El Ela, M. K. Elmously, K. S. Abdu, *Journal of Materials Science* **15**(4), 871 (1980).
- [11] Barták Jaroslav, Simona Martinková, Jiří Málek, *Crystal Growth & Design* **15**(9), 4287 (2015)
- [12] L. Blaine Roger, Homer E. Kissinger, *Thermochimica Acta* **540**, 1 (2012).
- [13] Matusita, Kazumasa, Takayuki Komatsu, Ryosuke Yokota, *Journal of Materials Science* **19**(1), 291 (1984).
- [14] Matusita, Kazumasa, Sumio Sakka, *Journal of Non-Crystalline Solids* **38**, 741 (1980).
- [15] Matusita, Kazumasa, Takayuki Komatsu, Ryosuke Yokota, *Journal of Materials Science* **19**(1), 291 (1984).
- [16] T. Ozawa, *Polymer* **12**(3), 150 (1971).
- [17] Cornelius T. Moynihan, Allan J. Easteal, James Wilder, Joseph Tucker, *The Journal of Physical Chemistry* **78**(26), 2673 (1974).
- [18] Málek Jiří, Takefumi Mitsuhashi, *Journal of the American Ceramic Society* **83**(8), 2103 (2000).
- [19] Anup Kumar, P. B. Barman, Raman Sharma, *Journal of Thermal Analysis and Calorimetry* **114**(3), 1003 (2013).
- [20] M. M. Heireche, M. Belhadji, N. E. Hakiki, *Journal of thermal analysis and calorimetry* **114**(1), 195 (2013).
- [21] Essam Shaaban, Ishu Kansal, M. Shapaan, José Ferreira, *Journal of thermal analysis and calorimetry* **98**(2), 347 (2009).
- [22] Zishan Husain Khan, Shamshad A. Khan, Numan Salah, Sami S. Habib, A. A. Al-Ghamdi, *Journal of Experimental Nanoscience* **6**(4), 337 (2011).
- [23] Mihai A. Popescu, *Non-Crystalline Chalcogenides* **8**, Springer Science & Business Media, 2001.
- [24] Syed Rahman, M. Venkata Ramana, G. Sivarama Sastry, *Journal of Materials Science Letters* **10**(13), 792 (1991).
- [25] Manish Saxena, Shilpa Gupta, *Materials Focus* **6**(4), 456 (2017).
- [26] Sunil Kumar, Kedar Singh, Neeraj Mehta, *Philosophical Magazine Letters* **90**(8), 547 (2010).
- [27] Sunanda Sharda, Neha Sharma, Pankaj Sharma, Vineet Sharma, *Journal of Alloys and Compounds* **611**, 96 (2014).
- [28] Jan Siegel, A. Schropp, Javier Solís Céspedes, Carmen N. Afonso, M. Wuttig, *Rewritable phase-change optical recording in Ge₂Sb₂Te₅ films induced by picosecond laser pulses*, (2004).
- [29] Sunil Kumar, Kedar Singh, Neeraj Mehta, *Philosophical Magazine Letters* **90**(8), 547 (2010).
- [30] Ravi P. Tripathi, Kedar Singh, Shamshad A. Khan, *Materials Chemistry and Physics* **211**, 97 (2018).
- [31] Faisal A. Al-Agel, Shamshad A. Khan, Esam A. Al-Arfaj, Ahmad A. Al-Ghamdi, *Journal of Non-Crystalline Solids* **358**(3), 564 (2012).
- [32] Shamshad A. Khan, M. Zulfequar, M. Husain, *Journal of Physics and Chemistry of Solids* **63**(10), 1787 (2002).
- [33] Anis Ahmad, Shamshad A. Khan, Zishan H. Khan, M. Zulfequar, Kirti Sinha, M. Husain, *Physica B: Condensed Matter* **382**(1-2), 92 (2006).
- [34] Xiang Shen, Qihua Nie, Tiefeng Xu, Shixun Dai, Xunsi Wang, Feifei Chen, *Physica B: Condensed Matter* **404**(2), 223 (2009).
- [35] S. S. Ashraf, M. Zulfequar, M. Uddin, *Chalcogenide Letters* **15**(4), 227 (2018).
- [36] Shamshad A. Khan, M. Zulfequar, M. Husain, *Solid state communications* **123**(10), 463 (2002).
- [37] Syed S. Ashraf, M. Zulfequar, Moin Uddin, *Recent Innovations in Chemical Engineering Formerly Recent Patents on Chemical Engineering* **11**(3), 172 (2018).
- [38] Sara A. Cortes, Miguel A. Muñoz Hernández, Hidetaka Nakai, Ingrid Castro-Rodriguez, Karsten Meyer, Alison R. Fout, Deanna L. Miller, John C. Huffman, Daniel J. Mindiola, *Inorganic Chemistry Communications* **8**(10), 903 (2005).
- [39] M. Zhang, S. Mancini, W. Bresser, P. Boolchand, *Journal of non-crystalline solids* **151**(1-2), 149 (1992).

- [40] Akihisa Inoue, Tao Zhang, Tsuyoshi Masumoto, *Materials Transactions JIM* **31**(3), 177990).
- [41], Z. P.Lu, H. Tan, S. C. Ng, Y. Li, *Scriptamaterialia* **42**(7), 667 (2000).
- [42]KeijiTanaka,*Physical Review B* **39**(2),1270 (1989).
- [43] K. A.Aly, Farid M. Abdel Rahim, A. Dahshan, *Journal of Alloys and Compounds* **593**, 283 (2014).
- [44] E. R.Shaaban, M. T. Dessouky, A. M. Abousehly, *Philosophical Magazine* **88**(7), 1099 (2008).
- [45], RyongJoonRoe, Wang Cheol Zin, *Macromolecules* **17**(2), 189 (1984).
- [46] F. Wang, Q. Liao, H. Zhu, Y. Dai, H. Wang, *J. Alloys Compd.* **686**, 641 (2016).
- [47] JiříMálek,*Thermochimicaacta* **267**, 61 (1995).
- [48] JiříMálek, TakefumiMitsubishi, *Journal of the American Ceramic Society* **83**(8), 2103 (2000).
- [49] JiříMálek,*Thermochimicaacta* **200**, 257 (1992).
- [50] Kazumasa Matusita, SumioSakka, *Journal of Non-Crystalline Solids* **38**, 741 (1980).
- [51] SudhaMahadevan, A. Giridhar, A. K. Singh, *Journal Of Non-Crystalline Solids* **88**, 11 (1986).
- [52] N. X.Sun, X. D. Liu, K. Lu, *ScriptaMaterialia* **34**(8), 1201 (1996).
- [53] MelvinAvrami,*The Journal of chemical physics* **7**(12), 1103 (1939).
- [54] Cornelius T.Moynihan, Allan J. Easteal, James Wilder, Joseph Tucker, *The Journal of Physical Chemistry* **78**(26), 2673 (1974).
- [55] C. T.Moynihan, S-K. Lee, M. Tatsumisago, T. Minami, *Thermochimicaacta* **280**, 153 (1996).
- [56] T. Ozawa, *Polymer***12**(3), 150 (1971).
- [57] Takeo Ozawa, *Bulletin of the chemical society of Japan* **38**(11), 1881 (1965).
- [58], Homer E. Kissinger,*Analytical chemistry* **29**(11), 1702 (1957).
- [59] Kazumasa Matusita, SumioSakka, *Journal of Non-Crystalline Solids* **38**, 741 (1980).